

## DIGITAL TWIN OF AN INTERNAL COMBUSTION ENGINE

Reza Ziarati, C4FF, UK, [reza.ziarati@c4ff.co.uk](mailto:reza.ziarati@c4ff.co.uk), Presenter Author

German De Melo Rodrigues, UPC, Spain, [germandemelo@gmail.com](mailto:germandemelo@gmail.com), Corresponding author

Lakhvir Singh, MariFuture, UK, [lakhvir.singh@c4ff.co.uk](mailto:lakhvir.singh@c4ff.co.uk); ITC Modeling

### Abstract:

*Major marine engine companies such as Wartsila have developed both their new 4-stroke and 2-stroke using gas and hence strongly believe that Internal Combustion Engines (ICE) have a place in marine power propulsion and auxiliary units. A recent announcement that Mazda sees a bright future for ICE is also indicative of the automotive industry has not lost hope in the future of ICE. This paper reports on recent developments to construct a digital twin of these power units with a view to improve their performance and also as a means of monitoring their behaviour when changes are introduced. This paper is composed of two parts. Part 1 is the digital half of an Internal Combustion Engine (ICE) which concerns the development of a mathematical model of the ICE and a suite of computer simulation programs which would allow the effects of various design and operational changes to be reliably and accurately predicted with the ultimate aim of producing cleaner engines and/or more efficient power units. The model has been tested against the experimental results of the Paxman engine at Newcastle University and earlier against the Atlas engine at Ricardo, Brighton, UK and most recently on the TUDEV Engine (2015). Part 2, contains the other digital half of the ICE which describes the rig developments viz., the physical model of an Engine. The key features of both Parts of the paper will be presented at the conference due to commercial confidentiality. However, the idea is to match the two parts using an earlier model developed by Ziarati (2009) to produce a finger print of both the mathematical model and the physical model. The matching of both parts would enable the mathematical model to be used for various design and operational changes with a view to reduce fuel consumption and/or engine harmful emissions. The predicted results and the experimental data are in good agreement.*

### Keywords:

*Digital Twinning, Internal Combustion Engines, Cleaner Diesel.*

### NOMENCLATURE

$s'$ : instantaneous stroke

$l$ : conrod length

$s$ : stroke

$V'$ : instantaneous volume

$M_T$ : trapped mass

$P_A$ : piston area

$\eta_v$ : volumetric efficiency  
 $V_{cl}$ : clearance volume  
 $R$ : gas constant  
 $\bar{d}$ : valve diameter  
 $\bar{l}$ : valve lift  
 $P_{in}$ : inlet pressure  
 $P_{ex}$ : exhaust pressure  
 $\rho_{in}$ : inlet density  
 $\rho_{ex}$ : exhaust density  
 $SR$ : scavenge ratio  
 $m$ : polytrophic index  
 $M_F$ : mass of fuel  
 $LHV$ : lower heating value  
 $A$ : flow area  
 $h_n$ : number of holes  
 $T_I$ : injection period  
 $d_n$ : injector hole diameter  
 $\theta$ : crank angle  
 $t_w$ : time at wall impingement  
 $V_f$ : fuel velocity  
 $C_n$ : mean piston speed  
 $Re$ : Reynolds number  
 $T_w$ : wall temperature  
 $FMEP$ : friction mean effective pressure  
 $ECHR[\text{cal/g}]$ : 1<sup>st</sup> law heat release  
 $P_2[\text{kPa}]$ : cylinder pressure  
 $TT_2[\text{K}]$ : combined cylinder temperature  
 $TAZ[\text{K}]$ : air zone temperature  
 $TBZ[\text{K}]$ : product zone temperature  
 $CHR[\text{cal/g}]$ : maximum possible heat release  
 $CQL[\text{cal/g}]$ : heat loss  
 $PWI[\text{kW}]$ : indicated power  
 $PWB[\text{kW}]$ : brake power  
 $TORQ [\text{Nm}]$ : brake torque  
 $IMEP [\text{kPa}]$ : indicated mean effective pressure  
 $BMEP [\text{kPa}]$ : indicated mean effective pressure  
 $SFCI[\text{kg/kWh}]$ : indicated specific fuel cons.  
 $SFCB[\text{kg/kWh}]$ : brake specific fuel cons.  
 $ANGPM[\text{degree}]$ : crank ang. at max. cylinder pres  
 $PMAX[\text{kPa}]$ : maximum cylinder pressure  
 $TMAX[\text{K}]$ : maximum cylinder temperature  
 $TEX[\text{K}]$ : exhaust temperature  
 $ETAM[\text{nd}]$ : mechanical efficiency  
 $DP[\text{kPa}]$ : initial pressure rise  
 $DT[\text{s}]$ : duration of initial pressure rise  
 $CCW[\text{kJ}]$ : compression and combustion work  
 $HTF[\text{nd}]$ : fraction of total heat lost  
 $FRCOM[\text{nd}]$ : fraction of fuel burnt  
 $EW[\text{kJ}]$ : expansion work

WBD[kJ]: blow down work  
 WEX[kJ]: exhaust work  
 WOL[kJ]: over lap work  
 WS[kJ]: suction work  
 VOL[cm<sup>3</sup>]: instantaneous cylinder volume  
 TEMP[K]: cylinder temperature

## INTRODUCTION

Calculating and analysing the performance characteristics of an engine before the production is a very cost and time effective process for engine manufacturers, especially for marine engine sector because of the size, cost and the production time of marine engines. For this reason computer simulation programs and mathematical models are very important research tools. Furthermore, the importance of reducing exhaust emissions cannot be overstressed. The reduction of diesel exhaust emissions at sea and in port has now become a major environmental issue with major national and international bodies promoting research to reduce these harmful pollutants.

The mathematical model developed has one main program and two auxiliary programs. The main program is called, “Element Mixing Program” which calculates cylinder pressure and hence engine performance parameters from combustion equations that leads to the calculation of heat release. The first auxiliary program is known as “Heat Release”, which calculates heat released in one engine cycle using experimentally measured cylinder pressure data. The second auxiliary program is called “Rate of Injection”. In this program the total mass of fuel injected into the cylinder in one engine cycle is obtained. The output for rate of injection is used as input data to the main program.

The main issue for the engine modelling is to calculate the fuel-air mixing process which is the fundamental part of the heat release. After calculating and understanding the heat release characteristic of the diesel engine, other parameters can be calculated easily.

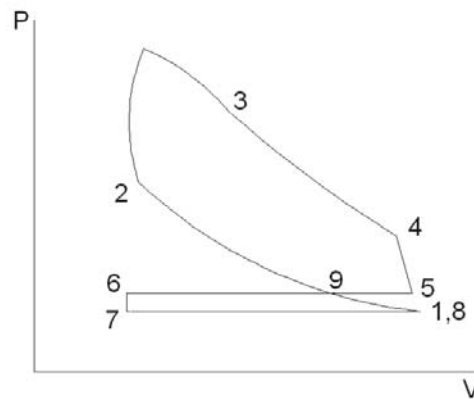
The main aim of this paper is to design and develop a clean diesel mathematical model and computer simulation program to predict the overall engine performance for changing load and speed parameters. The model should be able to respond to the changes in various parameters according to already established experimental trends and observations. The initial computer programs were developed by Ziarati (1991) and subsequently in revised Ziarati (1995). These programs were translated into FORTRAN programming language in 2007 and several changes were carried out in 2015.

In order to test the computer programs against experimental data, in 2008 a computer controlled engine rig was set up at TUDEV, Turkey. The intention is apply the programs and enable it also to predict the exhaust emissions (Ozkaynak, 2009). The tests were repeated in 2014 to ascertain use of diesel and gas combinations (Ashok et al, 2015; Ziarati and Akdemir, 2015). Due to commercial sensitivity, the type of fuel and engines used cannot be revealed but will be discussed at the conference. The results of 2014 engine test were compared with latest results by major engine manufacturers including Warsila’s new gas engine.

## 1 DESCRIPTION OF THE MODEL

The programs use the modified air standard cycle as shown in Figure 1.

**Figure 1 RZ Cycle - Generalised Air Standard Cycle representing Diesel, Carnot and Diesel/Gas cycles**



The RZ Cycle is subdivided into:

- a) Closed Cycle Considerations:
  - Compression period (1-2)
  - Combustion period (2-3)
  - Expansion period (3-4)
- b) Open Cycle Considerations:
  - Blow down period (4-5)
  - Exhaust period (5-6)
  - Overlap period (6-7)
  - Suction period (7-8)
  - Pre-compression period (8-9)

The model can be divided into two calculation parts: Analysis and Synthesis. The analysis part has its own program named “Heat Release Analysis Program”. The synthesis part is the “Element Mixing Program”.

### 1.1 ELEMENT MIXING PROGRAM

The model assumes that after injection the air entrainment is controlled by an elemental fuel jet until the wall impingement. After the injected fuel impinges to the wall the air entrainment is controlled by an elemental wall jet and close to this jet the intimate fuel air mixing within the jet is controlled by turbulent diffusion. The entrainment of the fuel jet and wall jet is controlled by entrainment ratio and micro mixing of the remaining fuel by

diffusivity constant. These values are dependent on engine load, speed and boost depending on the application. The model can be used to predict heat release qualitatively for any direct injection engine using estimated values of the diffusivity constant and entrainment ratio.

The mixing of air with the injected fuel in the combustion chamber is directly proportional to the air entrainment by the fuel jet at any instant quantities. Micro mixing of fuel and air depends on a simple consideration of turbulent diffusion. This expression includes an Arrhenius type function which controls the rate of burning (micro mixed fuel and air). The following assumptions are made:

- The molar change of the cylinder content is negligible before, during and after combustion
- During combustion, that is, during the period of heat release, the increase in the internal energy is based on the data (Gilchrist, 1947) which takes into account the effect due to changes of specific heat and dissociation. Hence, in considering internal energy and specific heat, dissociation has to be taken into account although the effect of its molar change on pressure and volume may be neglected.

#### 1.1.1 OBJECT OF THE PROGRAM

The total fuel injected is divided into a number of elements and the individual fuel-air mixing history of each element is calculated independently using the model. From these histories an aggregate mixing condition can easily be calculated and from this latter the cylinder pressure and heat release are determined (Ziarati, 1991).

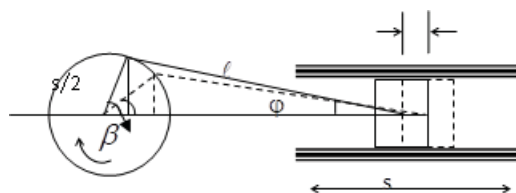
#### 1.1.2 PRE-COMPRESSION CONSIDERATION AND COMPRESSION PERIOD

The compression period starts from the initial atmospheric conditions. The compression process is assumed to obey the rule:

$$PV^n = \text{constant} \quad (1)$$

Assuming compression starts at bottom dead centre, the crank angle dependent volume can be calculated as follows (Heywood, 1988):

**Figure 2 Piston Travel**



$$s' = l + (s/2) - (l \cos \phi + (s/2) \cos \beta) \quad (2)$$

$$V' = s' \cdot \text{piston area} \quad (3)$$

Then the trapped mass must be calculated at point 1. The following two methods can be used:

- Simplified perfect displacement model:

$$M_T = (s \cdot P_A \cdot \eta_v + V_{cl} \cdot \frac{T_1}{T_{exh}}) \frac{P_1}{R \cdot T_1} \quad (4)$$

- Simplified perfect mixing model:

$$M_T = (s_{eff} \cdot P_A + V_{cl}) \frac{P_1}{R \cdot T_1} \quad (5)$$

The air flow through the clearance volume during the scavenge period is given by:

$$\dot{V}_a = 2 \cdot \pi \cdot \bar{d} \cdot \bar{l} \cdot \sqrt{\left( \frac{P_{in} - P_{ex}}{\rho_{in} - \rho_{ex}} \right)} \quad (6)$$

For perfect mixing the scavenge efficiency:

$$\eta_s = 1 - e^{-SR} \quad (7)$$

After calculating scavenge efficiency, the loss of air to exhaust and trapped residual gases can be calculated. The inlet temperature can be modified using the universal gas equation;

$$T_1 = \frac{P_1 \cdot V_1}{M_T \cdot R} \quad (8)$$

So the temperature at start of injection;

$$T_2 = T_1 \cdot \left( \frac{V_1}{V_2} \right)^{m-1} \quad (9)$$

Compression work,

$$W_{1-2} = P_1 \left[ V_1 - V_2 \cdot \left( \frac{V_1}{V_2} \right)^m \right] \cdot 10^{-6} \quad (10)$$

Other parameters calculated at this stage are as follows:

Air-fuel ratio;

$$R_T = \frac{M_T}{M_F} \quad (11)$$

Total heat input per unit mass of air,

$$H_i = \frac{LHV}{R_T} \quad (12)$$

Fractional air utilization:

$$U' = \frac{R_{stoich}}{R_T} \quad (13)$$

Applying the momentum equation (Bernoulli's equation) the overall mean injection pressure is also calculated as follows:

Volumetric flow rate,

$$\dot{Q} = KA \sqrt{\frac{2\Delta P}{\rho_f}} \quad (14)$$

Therefore;

$$M_F = \dot{Q} \rho_f \frac{T_I}{6\text{RPM}} \quad (15)$$

Thus

$$\Delta P = 71,0433.10^{-6} \left[ \frac{M_F \text{RPM}}{h_n T_I d_n^2} \right]^2 \quad (16)$$

Before the start of combustion, air zone temperature is equal to product zone temperature and is given by:

$$\text{TAZ} = \text{TBZ} = T_1 \left( \frac{V_1}{V_2} \right)^{m-1} \quad (17)$$

This leads to the evaluation of the internal energy of the compressed air using the given Gilchrist Table (Gilchrist, 1947) and the gas constant function. There are two periods: The period of pre-mixed combustion and rate of pressure rise (and therefore initial rate of heat release) is governed by the quantity of fuel injected during the delay period. In the second period, the burning is controlled by the mixing rate which has an empirical expression.

### 1.1.3 Free Jet

The fuel injected first forms a free jet and may later form an axi-symmetric wall jet. For a given step, rate of injection is assumed constant, and the position of free jet at time 't' since the beginning of injection is assumed to be governed by the following equation (Ziarati et al., 1988):

$$y = 1020, 8 \left( \frac{d_n P_{i1/2} \rho_{\text{stpt}}}{\rho_c} \right)^{1/2} \quad (18)$$

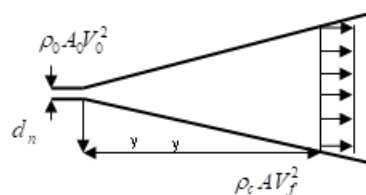
Application of momentum equation leads to:

$$\Delta E = \int_t^{t+\Delta t} \frac{\pi}{3} \tan^2 \theta y^3 \rho_a dt \quad (19)$$

Integrating equation (19) and using equation (18) lead to:

$$\Delta E = \frac{\pi}{3} \rho_a \tan^2 \theta \left[ \frac{1,042.10^6 d_n P_{i1/2} \rho_{\text{stpt}}}{\rho_c} \right]^{3/2} [(t + \Delta t)^{3/2} - t^{3/2}] \quad (20)$$

Figure 3 Spray Presentation (Ziarati, 1991)



### 1.1.4 WALL JET

Once  $t$  is greater than  $T_Y$  (impingement time) the jet front changes from a free jet to a wall jet (Ziarati et al., 1988). Transition time, air entrainment during transition and loss of kinetic energy in the direction of flow for the transition are neglected. The initial conditions for the wall jets are:

$$r_0 = Y \tan \theta \quad (21)$$

and since the velocity and flow areas immediately before and immediately after transition are assumed to be the same, initial volume flow at wall jet can be found:

$$\begin{aligned} Q_0 &= \pi r_0^2 W_0 \\ Q_0 &= \pi y^2 \tan^2 \theta W_0 \end{aligned} \quad (22)$$

The equation of Glauert (Glauert, 1956) is now can be used to describe the velocity  $W$ , jet thickness and volume flow  $Q$  (of the wall jet) assuming again a square velocity profile for the jet front,

$$\Delta E_{\text{wall}} = \frac{Q_0 \rho_a}{1,459 t_0^{0,459}} [(t_w + \Delta t)^{1,459} - t_w^{1,459}] \quad (23)$$

After the end of the injection the net increment in air entrainment is then:

$$\Delta E = \Delta E_{\text{jetfront}} - \Delta E_{\text{jetback}} \quad (24)$$

Further, the jet is assumed to expand or contract with cylinder volume.

### 1.1.5 MICRO MIXING

While the air entrained by the gas jet at any instant quantifies the larger scale mixing of fuel and air in the chamber, intimate mixing of fuel and air is represented by a simple consideration of turbulent diffusion. The macro mixed quantity of air within the jet boundaries, as determined by air entrained  $E$  is assumed to micro mix with injected fuel according to the equation:

$$\frac{dM_a}{dt} + DV_f M_a = DV_f E \quad (25)$$

Multiplying both sides of the equation by  $e^{DV_f t}$  and integrating:

$$M_a e^{DV_f t} = E e^{DV_f t} + c \quad (26)$$

Heat release therefore;

$$H_{\text{release}} = \frac{M_a \text{LHV}}{15} \quad (27)$$

## 2.2 Combustion Work Done

The combustion work can be obtained from the 1<sup>st</sup> law of thermodynamics (Heywood, 1988, Ferguson, 1986) as follows:

$$W_{2-3} = W_{\text{combustion}} \quad (28)$$

### 1.2 DELAY PERIOD

With the following empirical expression, the delay period can be calculated (Ziarati, 1990):

$$\text{DEL} = 15,375 \cdot 10^{-3} \text{RPM} (C_n)^{-a} (P)^{-0,38} e^{AE/T} + 39,04 \Delta P^{-0,35} d_n^{0,4} \quad (29)$$

Where  $a=0,7$  to  $1,0$  and  $AE$  is the activation energy.

### 1.3 HEAT TRANSFER

The heat transfer formula used in the model is Annand's based on the actual cylinder piston surface areas and is calculated step by step throughout the calculations (Annand, 1963). This equation can be expressed as follows:

$$\dot{q} = A \frac{aK}{D} (\text{Re})^b (T - T_w) + c(T^4 - T_w^4) \quad (30)$$

### 1.4 WORK DONE

Expansion work: The expansion process starts from the condition at the end of combustion and this period is the last sequence of closed cycle calculations. The expansion work (Heywood, 1988, Ferguson, 1986):

$$W_{3-4} = \frac{(P_3 V_3 - P_4 V_4)}{n-1} \cdot 10^{-6} \quad (31)$$

Closed period work done: Closed period work done is the total work of the processes 1-2, 2-3 and 3-4:

$$W_{1-4} = \int_1^4 P dv = W_{1-2} + W_{2-3} + W_{3-4} \quad (32)$$

Blown-down period work done:

$$W_{4-5} = \frac{P_4 - P_5}{2} (V_5 - V_4) \quad (33)$$

Exhaust period work done:

$$W_{5-6} = -P_6 (V_6 - V_5) \quad (34)$$

Overlap period work done:

$$W_{6-7} = -P_5 (V_6 - V_{cl}) + P_7 (V_7 - V_{cl}) \quad (35)$$

Suction period work done:

$$W_{7-8} = P_7 (V_8 - V_7) = P_7 (V_5 - V_7) \quad (36)$$

Pre-compression work:

$$W_{4-8} = \int_4^8 P dv = W_{4-5} + W_{5-6} + W_{6-7} + W_{7-8} \quad (37)$$

### 2.6 Overall Cycle Parameters:

$$W_{ind} = W_{closedperiod} + W_{openperiod} \quad (38)$$

Since the friction mean effective pressure is generally known, the brake work is given by:

$$W_{brake} = W_{ind} - \text{FMEP} \cdot V_{swept} \quad (39)$$

The power output indicated and brake can be calculated respectively as:

$$P_{ind} = W_{ind} \cdot \text{RPM} \quad (40)$$

$$P_{brake} = W_{brake} \cdot \text{RPM} \quad (41)$$

Similarly, specific fuel consumption is given by:

$$\text{SFCI} = \frac{\text{RPM}M_F}{P_{\text{ind}}} \quad (42)$$

And

$$\text{SFCB} = \frac{\text{RPM}M_F}{P_{\text{brake}}} \quad (43)$$

The computer program represents equations (1) to (43) with some exceptions and additional complications and facilities (Ziarati, 1991).

## 2 HEAT RELEASE PROGRAM

The basis of this “Heat Release” program depends on the 1<sup>st</sup> law of thermodynamics (Heywood, 1988, Ferguson, 1986):

$$Q - W = U \quad \text{Therefore:} \quad (44)$$

$$Q = \int_B^{AB} Pdv + U$$

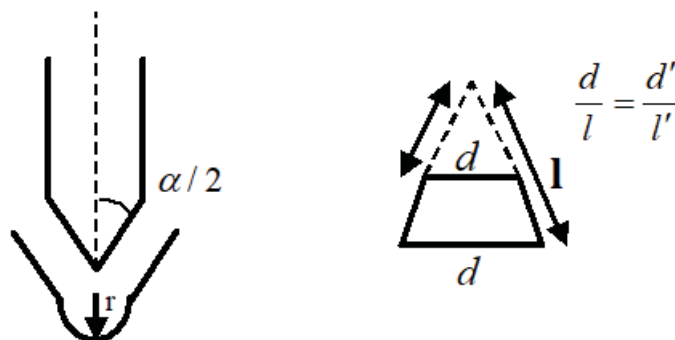
## 3 RATE OF INJECTION PROGRAM

This program can be used only when practical injection diagrams are considered. Rate of injection program calculates the rate of fuel injected at specified crank angle. The annular area between the needle and the seat and total nozzle holes area are assumed to be two orifices in series. Knowledge of the line pressures  $P_L$ , cylinder pressures  $C_P$  and needle lifts  $L$  for specified crank angles for any given step enables the rate to be calculated:

$$Q = K_e A'_e \sqrt{(P_{\text{diff}}/\text{RPM})} \quad (45)$$

$Q$  can therefore be calculated for each element. The equation (45) can only be correctly determined if  $A_s$  and  $A_h$  can be calculated as shown:

Figure 4 Valve Seat Presentation (Ziarati, 1991)



If the seat angle is assumed to be  $60^\circ$ , the truncated cone  $A'_s$  equals to:

$$A'_s = \frac{\pi}{2} dl - \frac{\pi}{2} d'l'$$

$$= \frac{\pi}{2} (dl - d'l') \quad (46)$$

Thus,

$$A'_s = \pi L \sin(\alpha/2) [d - L \sin(\alpha/2) \cos(\alpha/2)] \quad (47)$$

Assuming  $d = d'$  and  $\alpha = 60^\circ$ ,  $A'_s$  expression reduces to:

$$A'_s = \pi r_{\text{sac}} \cdot L \quad (48)$$

#### 4 VALIDATION OF THE PROGRAMS

The developed model was applied to a single cylinder direct injection diesel engine (Ricardo, Atlas) for a number of nozzle configuration, plunger sizes, engine speeds and engine loads. The experimental heat release data was available. Engine dimensions are below:

**Table 1 Research Engine Specifications.**

No. of Cylinders	1
Bore	215.9 mm
Stroke	241.3 mm
Swept Volume	8833 mm <sup>3</sup>
Compression Ratio	11
Inlet Valve Opening	48 deg CA

**Table 2 Theoretical and Experimental Results (Ziarati, 1991).**

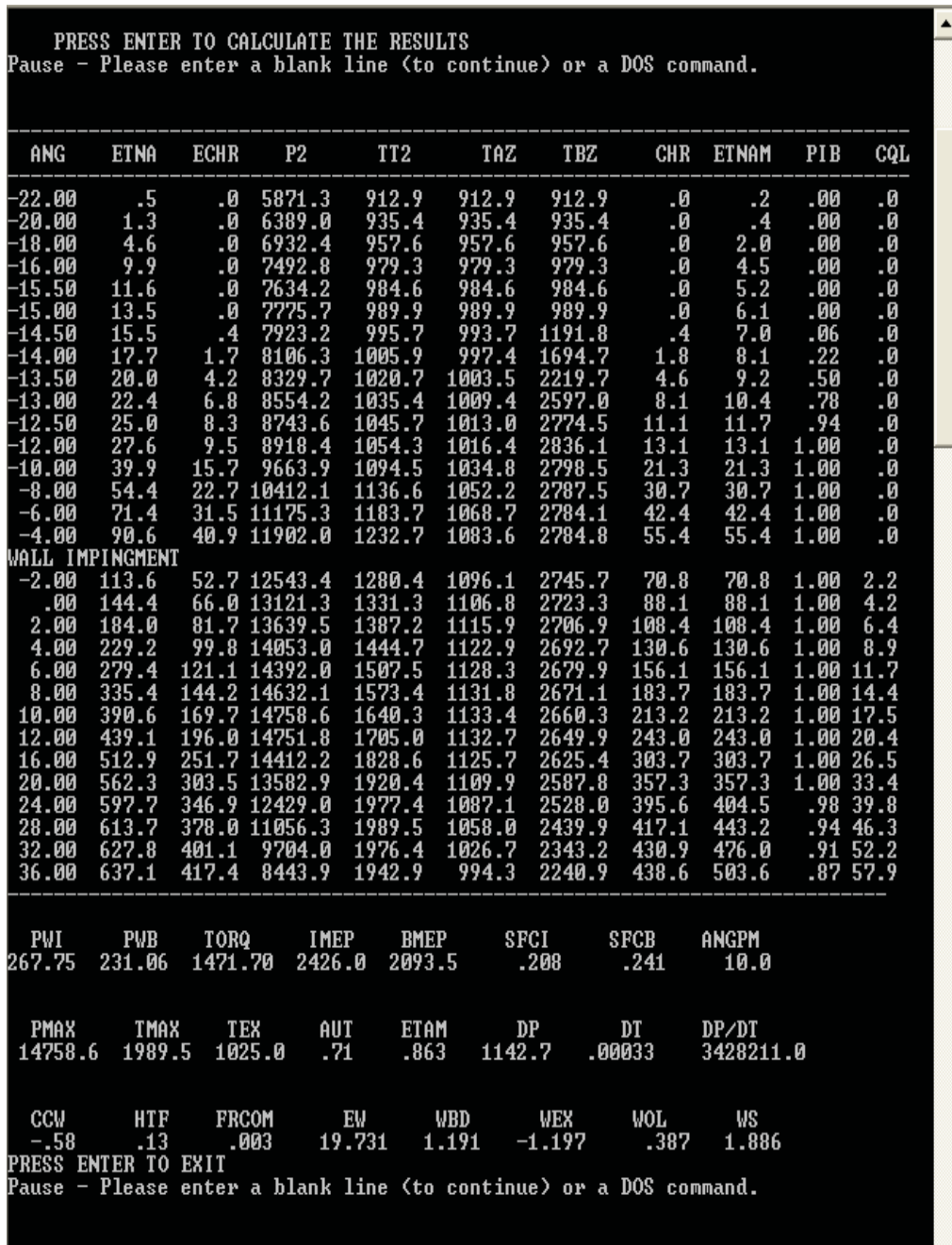
					Experimental				Theoretical			
Plunger (mm)	Nozzle config.	Boost (bar)	Scavenge ratio	Speed (rpm)	Bmep (bar)	Bsfc (kg/kWh)	Isfc (kg/Kwh)	Pmax (bar)	Bmep (bar)	Bsfc (kg/kWh)	Isfc (kg/kWh)	Pmax (bar)
22	8x0,40	3,0	1,05	1500	17,91	261,5	193,8	146	17,88	263	195	144,3
22	9x0,35	2,12	1,05	1500	10,84	274,9	174,4	115	10,83	276	174,7	113,3
22	9x0,45	2,12	1,05	1500	10,83	291	184,5	115	10,65	296	187	114,2
22	9x0,35	3,0	1,05	1200	19,48	240,6	194,6	145	18,77	250	201	144,9
20	9x0,40	3,0	1,05	1500	17,78	274,7	203,5	146	17,90	274	203	142,7
20	9x0,40	3,6	1,1	1500	17,78	281,5	208,3	145	18,03	277	206	143,0
20	9x0,40	3,0	1,0	1000	20,56	249,4	213,1	146	20,04	256	218	144,2
20	9x0,40	3,6	1,05	1000	20,56	244	208,5	147	20,66	243	207	145,2
20	8x0,35	3,6	1,05	1200	19,54	242,9	196,6	149	19,56	243	196	148,6
20	8x0,35	3,6	1,05	1200	5,11	329,5	173,5	73	5,1	331	174	76,5
18	8x0,45	3,0	1,05	1500	17,67	282,7	208,8	147	17,90	282	209	143

Table 2 above summarizes the theoretical and experimental results for various conditions.

The test data sets are taken from previous works.

The screenshots of outputs from “Element Mixing Program”, “Heat Release Program” and “Rate of Injection Program” can be seen in Figures 5, 6 and 7 respectively:

Figure 5 Output Screenshot of Element Mixing Program.



As can be seen from Figure 5, all necessary outputs are calculated and cylinder pressure, cylinder temperature, heat release data are predicted. Also, wall impingement time, heat loss and air entrainment are shown.

Heat release program calculates the heat released by using experimental cylinder pressure data according to 1<sup>st</sup> Law of Thermodynamics. From Figure 6 it can be seen that fuel injection starts at 163 degrees CA, because the heat release is zero before that crank angle. After the injection heat release is going below zero, this is because the fuel absorbs energy from its environment to evaporate. After evaporation the heat release increases.

In Figure 6 the work done is decreasing in the compression period. But after top dead centre (180 degrees CA) it starts to increase due to the expansion period.

Figure 6 Output Screenshot of Heat Release Program.

RESULTS							
HEAT RELEASE CALCULATION CYCLE= 9							
CA	CYL P	UOL	TEMP	HEAT R	WORK D	DQ	DW
161.0	977.0	1109.6	941.0	.00	.00		
162.0						.611	-1.910
163.0	1063.0	1046.7	965.8	1.22	-3.82		
164.0						-1.013	-1.839
165.0	1132.9	990.4	973.9	-.80	-7.50		
166.0						.108	-1.730
167.0	1214.6	940.9	992.0	-.59	-10.96		
168.0						.843	-1.597
169.0	1299.8	898.2	1013.5	1.10	-14.15		
170.0						5.710	-1.453
171.0	1432.7	862.5	1072.6	12.52	-17.06		
172.0						.374	-1.255
173.0	1500.7	833.7	1086.1	13.27	-19.56		
174.0						5.693	-1.007
175.0	1619.2	812.0	1141.4	24.65	-21.58		
176.0						6.000	-.727
177.0	1729.1	797.5	1197.0	36.65	-23.03		
178.0						5.850	-.395
179.0	1822.8	790.0	1250.0	48.35	-23.82		
180.0						7.469	-.018
181.0	1916.5	789.7	1313.7	63.29	-23.86		
182.0						7.957	.396
183.0	1993.2	796.5	1378.1	79.20	-23.06		
184.0						7.435	.836
185.0	2036.6	810.4	1432.7	94.07	-21.39		
186.0						8.435	1.284
187.0	2065.8	831.5	1491.0	110.94	-18.82		
188.0						11.068	1.742
189.0	2100.0	859.6	1566.9	133.08	-15.34		
190.0						10.935	2.198
191.0	2107.3	894.7	1636.6	154.95	-10.94		
192.0						12.227	2.635
193.0	2105.1	936.7	1711.7	179.40	-5.67		
194.0						9.659	3.031
195.0	2061.3	985.6	1763.6	198.72	.39		
196.0						10.255	3.372
197.0	2010.2	1041.2	1816.9	219.23	7.13		
198.0						9.809	3.668
199.0	1945.5	1103.5	1863.6	238.85	14.47		
200.0						8.246	3.902
201.0	1863.7	1172.4	1896.7	255.34	22.27		
202.0						7.220	4.072
203.0	1773.4	1247.6	1920.6	269.78	30.42		
204.0						6.992	4.192
205.0	1683.1	1329.1	1941.9	283.76	38.80		
207.0						4.862	4.274
209.0	1488.1	1510.3	1950.9	303.21	55.90		
210.0						4.639	4.265
211.0	1398.3	1609.6	1953.7	312.49	64.43		
212.0						4.370	4.232
213.0	1313.5	1714.5	1954.7	321.23	72.89		
214.0						3.319	4.173
215.0	1230.0	1824.7	1948.2	327.87	81.24		
216.0						1.424	4.080
217.0	1144.8	1940.2	1928.1	330.72	89.40		

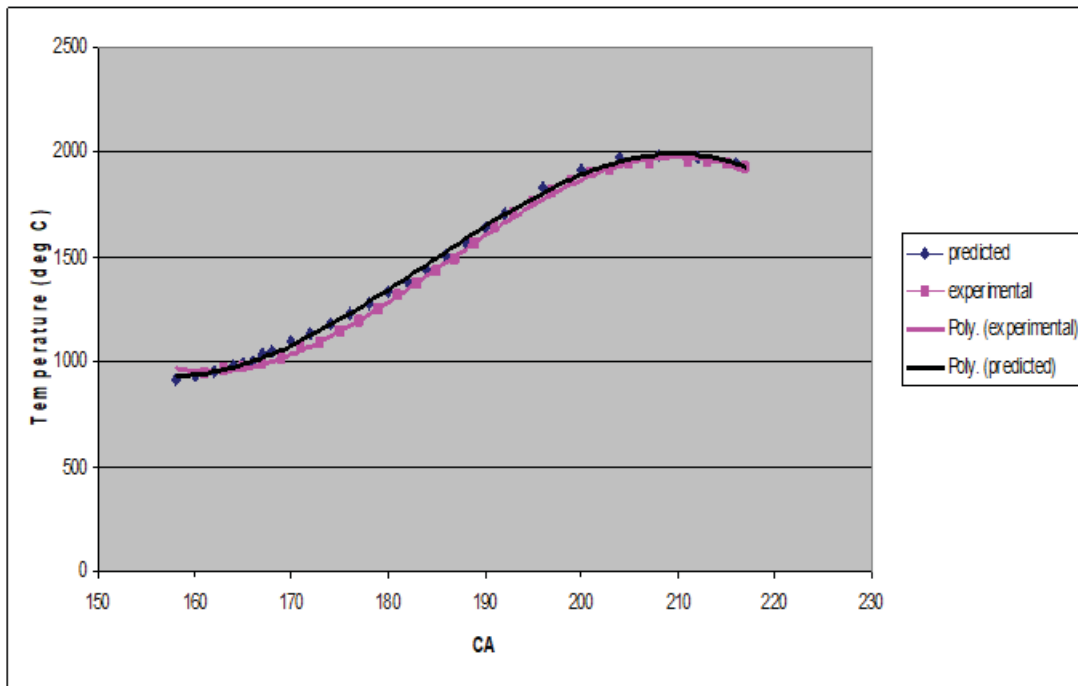
Figure 7 Output Screenshot of Rate of Injection Program.

RESULTS						
FUEL INJECTOR CALCS CYCLE= 9 CORRECTION FACTOR= 1.0806						
CA	FLOW R	ACC R	PN	CYL P	LINE P	LIFT
161.0	.1465	.0000	.05	977.00	3857.08	.0011
163.0	8.4172	8.5637	176.86	1063.03	5106.50	.0555
165.0	23.9945	40.9755	1437.23	1132.88	4632.05	.2224
167.0	34.3157	99.2856	2939.60	1214.65	4910.09	.5550
169.0	40.3377	173.9390	4061.87	1299.83	6270.72	.5994
171.0	41.2289	255.5057	4243.33	1432.70	6625.67	.5994
173.0	43.2576	339.9921	4671.19	1500.68	7217.25	.5994
175.0	48.5308	431.7805	5879.47	1619.25	8814.50	.5994
177.0	52.5062	532.8176	6882.16	1729.13	10151.47	.5994
179.0	52.6565	637.9803	6921.61	1822.82	10293.45	.5994
181.0	53.0989	743.7357	7038.41	1916.52	10530.08	.5994
183.0	53.9499	850.7845	7265.80	1993.18	10885.03	.5994
185.0	53.2027	957.9371	7065.95	2036.62	10683.89	.5994
187.0	52.3603	1063.5000	6843.96	2065.75	10441.34	.5994
189.0	50.3854	1166.2460	6337.41	2099.99	9855.68	.5994
191.0	45.4504	1262.0810	5156.77	2107.32	8418.15	.5994
193.0	40.4307	1347.9630	4080.61	2105.10	7098.93	.5994
195.0	27.9891	1416.3820	1955.60	2061.32	4454.58	.5994
197.0	16.7099	1461.0810	697.03	2010.22	2863.24	.5994
199.0	10.5102	1488.3020	275.76	1945.48	2307.15	.4995
201.0	9.0551	1507.8670	204.69	1863.71	2336.73	.2331
203.0	.0000	1516.9220	.00	1773.42	1478.94	.0011

PRESS ENTER TO EXIT  
 Pause - Please enter a blank line (to continue) or a DOS command.

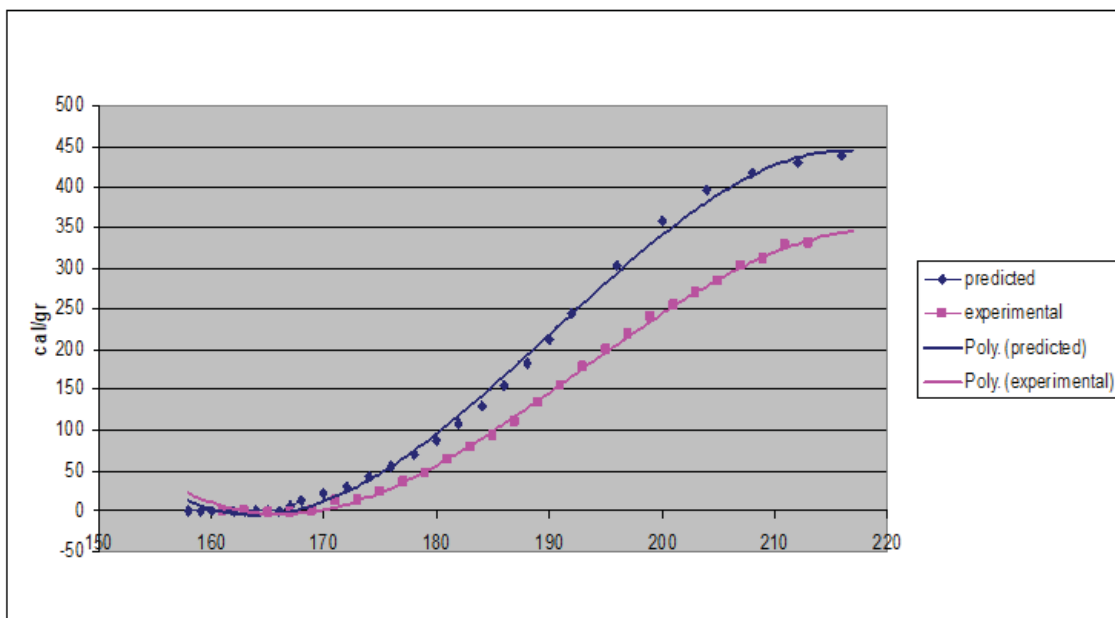
The predicted cylinder temperature against the experimental cylinder temperature calculated from “Heat Release Program” is shown in Figure 8 below:

Figure 8 Predicted and Experimental Cylinder Temperature.



The graphical comparison of predicted heat release and experimental heat release data for a given engine condition is shown in Figure 8. The predicted heat release is gross heat release which includes the heat loss so the differences between the predicted and experimental results are the heat loss.

**Figure 9 Predicted and Experimental Heat Release.**



## 5 ENGINE RIG DESIGN

The application of diesel engines in automotive and marine industries and its use as stand alone power units have been rapidly increasing in recent years mainly due to the development and applications of new technologies. These developments on diesel engines are focused on the performance increase and the emission control. To increase the performance, higher thermal efficiency and to control the emission, lower toxic gases

are targeted. Improving diesel engine performance and reducing exhaust emissions as well as using environmental friendly fuels have become important research topics recently. Therefore, a reliable and functional diesel engine test unit is required to perform research and train maritime cadets.

Rillings et al (1973) developed a computer controlled diesel engine test unit to carry out the transient analysis of an automobile engine. A mini computer was used for data acquisition and closed loop control of the dynamometer. The dynamic process provided real time data acquisition, logging and graphically presentation. Campell et al (1985) designed a low cost computer aided engine test unit. It was aimed to provide students for research facilities. Hydraulics dynamometer flow rate was controlled by an electric motor and various temperatures were logged in a PC. Williamson&Al-Khalidi (1989) tested internal combustion engines for only torque and power measurements at full throttle using dynamometers converting mechanical energy to heat. Kawarabayash (1990) aimed to improve a test stand control system. In this system, load transition was made faster and smoother. Voigt (1991) developed enhanced test laboratory to test an engine under various road conditions. In this test unit, computer based data acquisition and real time dynamometer control system were used. Turley&Wright (1997) developed a test automation system using Labview® for air craft engine tests. They selected Labview® due to its powerful tools such as measurement, data acquisition, appearance and preparing general algorithm which allows users to rapid prototype. Schmidt (1998) examined the vehicle model and effects of environmental factors. In the other test unit, electric motor was used to apply real load value based on the vehicle model. Plint&Martyr (2002) developed a standard test unit to measure torque, power, speed, temperature and emission. In addition to these, noise, vibration and cylinder pressure were measured. Celik et al. (2007) designed a diesel engine test unit developing a user interface algorithm. Due to convenience of the user interface, students could operate and test easily.

In this study, a computer controlled diesel engine test laboratory was established at Piri Reis University. The research facility is fully instrumented using a range of sensors and a computerized data processing and analysis system. The research rig is capable of computing diesel engine performance characteristics. The laboratory is separated into two facilities, one holding the instrumented engine and the other computing and display units with a view to improve safety and to decrease noise. Analogue, digital controls and measurement signals supplied by sensors and actuators in the engine room are conditioned by data acquisition card. The required data are displayed on the graphical user interface using Labview® and logged by transferring signals from the engine room to the computerized engine control room.

## **6 THE TEST ENGINE SETUP AND INSTRUMENTATION**

The research facility is fully instrumented using a range of sensors and a computerized data processing and analysis system and it is capable of computing diesel engine performance characteristics. The laboratory is separated into two rooms, one holding the instrumented engine and the other computing and display units with a view to improve safety and to decrease noise for researchers and students.

In the engine room, Antor 4LD820 single cylinder diesel engine is used and it is head to head coupled to a shunt excited DC generator which is used to load the Diesel engine. The electrical power produced by the generator is consumed by external load resistances.

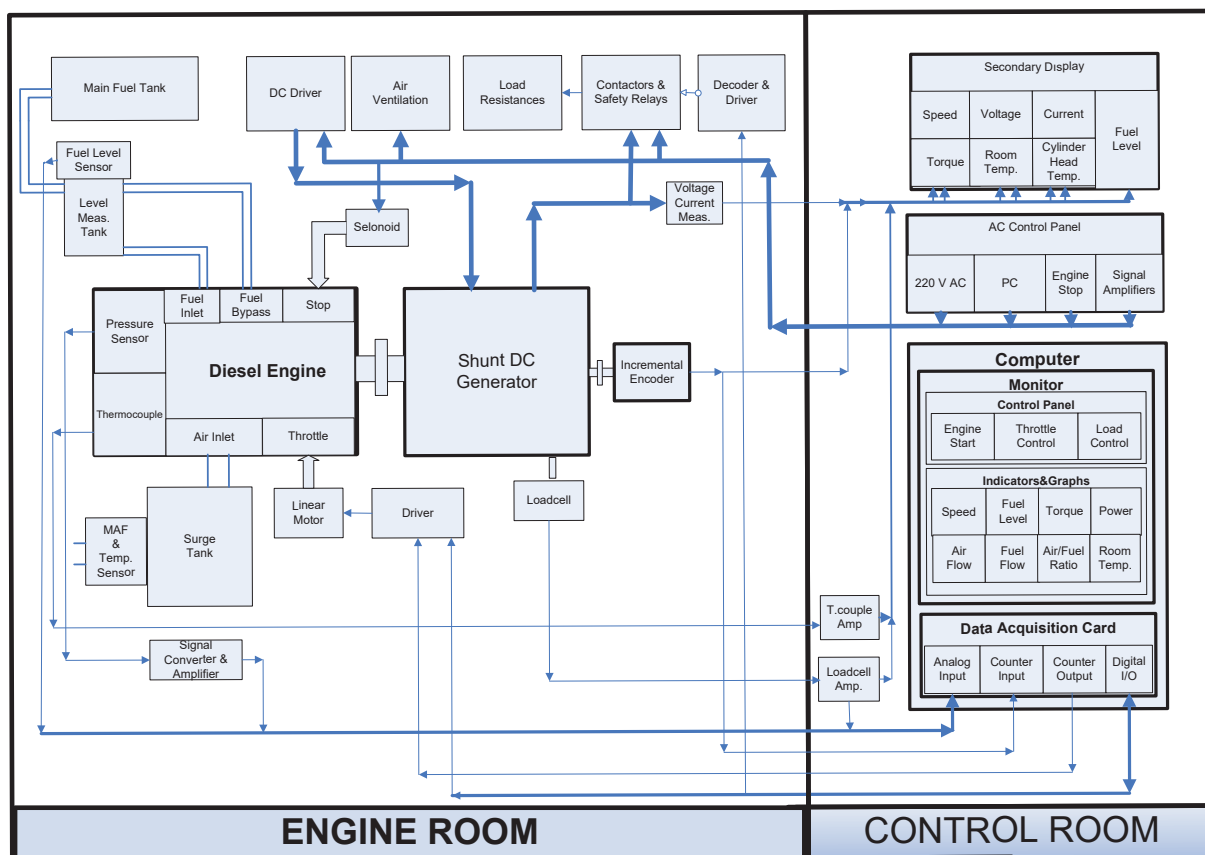
The cylinder pressure and cylinder head temperature are measured by a piezoelectric pressure sensor and a thermocouple which are mounted on the cylinder head. A mass air flow meter (MAF) is used to measure air flow rate and inlet air temperature. Fuel flow measurement is accomplished by a level sensor which floats in the cylindrical fuel tank with 5 cm diameter. An incremental encoder is coupled to engine shaft to measure engine speed and crank angle. Also, a load cell mounted on the DC generator body is used to measure the engine torque.

All control systems including engine start-stop, throttle and load buttons are located in the control room. Therefore, users can operate the whole system easily without entering the engine room. An operation system for the engine starter motor is designed and it stops automatically after the engine reaches a given speed. Throttle is controlled by a micro stepping motor with linear actuator. A decoder, a driver and contactors are used to control the number of resistances to load the engine. Diesel engine can be stopped with the help of a solenoid. Data acquisition card is used to acquire signals and generate control signals. With appropriate wiring to pins of counter/timer, digital and analog inputs/outputs, all signals are transferred between engine room and control room. Specifications of the Diesel engine, DC-generator, piezoelectric sensor and data acquisition card are given in Table 3.

**Table 3 Specifications of the engine, generator, piezoelectric sensor and data acquisition card.**

Diesel Engine		Generator		Piezoelectric Sensor	
Model	Antor 4LD 820	Type	Shunt DC	Manufacturer	Kistler
Nr.Of Cylinder	1	Max. Armature Current	38 A	Type	6061B
Displacement	817 cm <sup>3</sup>	Max. Armature Power	15 kw	Meas. range	0..250 bar
Engine RPM	2600(3000) rpm	Field Voltage	200 V	Sensivity	25 pC/bar
Power	15(17) HP	Field Current	2,8 A	Natural freq.	90 KHz
Max. Torque	5 Kg-m @1600 rpm	Max. Revolution	4000 rpm	Cooling	water
<b>Data Acquisition Card</b>					
Manufacturer	National Instruments	Analog Input		Digital I/O	
Model	PCI-6221	Number of Channels	16 SE/8DI	Nr of Channels	24
Measurement Type	Digital, Frequency, Encoder, Voltage	Sample Rate	250 kS/s	Max.Clock Rate	1 MHz
Counter/Timers		Resolution	16 bits	Logic Levels	TTL
Nr of Counter	2	Max. Voltage Range	-10...10V	Timing	Hardware
Resolution	32 bits	Resolution	16 bits	Logic Levels	TTL

**Figure 10. Block diagram of the laboratory.**



A dual-core cpu computer and two 19” monitors are used in the control room. A user friendly user interface algorithm was prepared using Labview ® which has flexible, powerful and attractive tools for algorithm design. Block diagram of the laboratory is shown in Fig. 10. In addition to that emission measurement devices were set up to measure and track the values of CO, NO<sub>x</sub>, CO<sub>2</sub>, O<sub>2</sub> and THC at the various diesel engine operating conditions. Technical specifications of the emission measurement devices are given in Table 4.

**Table 4 Specifications of the emission measurement devices.**

<b>Manufacturer&amp;Model</b>	Siemens,Ultramat 23			<b>Manufacturer&amp;Model</b>	Siemens, Fidamat 6
<b>Technique</b>	Non-dispersive Infrared			<b>Technique</b>	Flame ionization detection
<b>CO</b>	<b>NOx</b>	<b>CO2</b>	<b>O2</b>	<b>Total Hydrocarbons</b>	
0-2500 ppm	0-2500 ppm	0-25 %	0-25 %	0-10000 ppm	

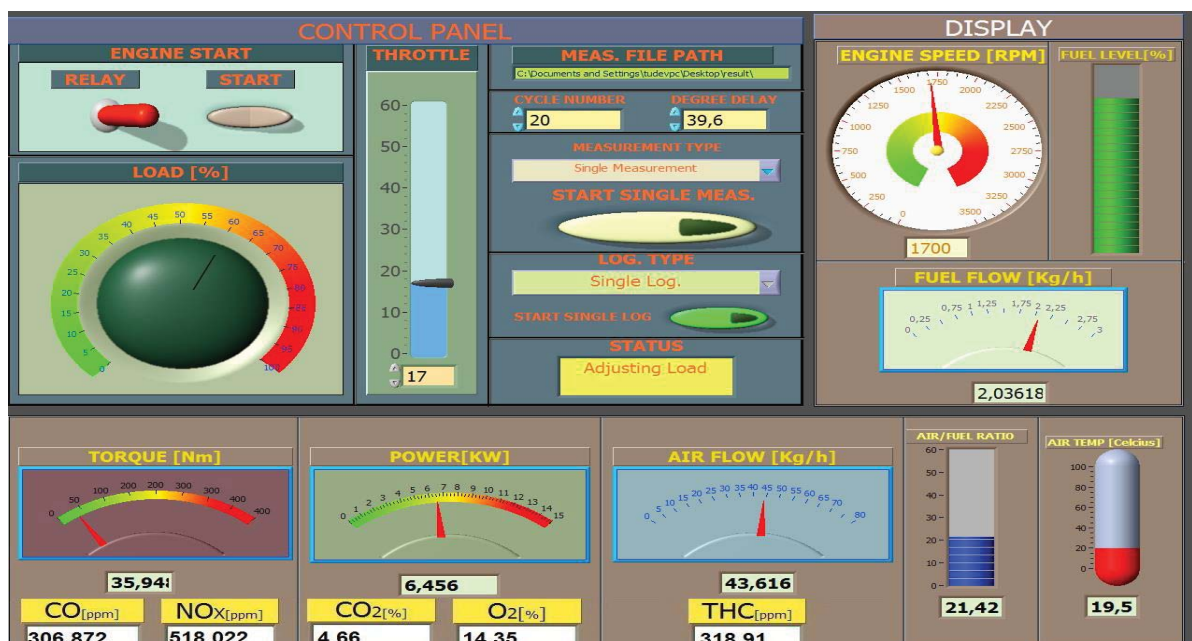
## 7 GRAPHICAL USER INTERFACE

A graphical user interface program was developed using Labview® (Travis, J. and Kring J. 2007). This program has several control functions and it displays measurement results and records the data on the hard disk. The graphical user interface consists of three parts; a control panel, indicator panel, and chart panel. Each panels were selected in different colors. The buttons of engine start, load control, throttle control, measurement results

saving path, cycle number, measurement type (continuous-single), and measurement record type (continuous-single) are installed on the control panel. Users can see and log data immediately after adjusting throttle and load by selecting measurement type (continuous or single). The user interface also provides two logging options as continuous and single, these measured data are stored in an .xls file.

Buttons of engine speed (rpm), fuel level (%), fuel flow (kg/h), air flow rate(kg/h), air/fuel ratio, torque (Nm), power (kW), air temperature (°C), status window are installed on the indicator panel. To take the exact value of the data both numerical and analog results are displayed on the panel at the same time. The indicator panel is refreshed after all measurements completed. Status window provides users instructions and information about progress. The indicator and control panels are shown in Fig.11.

Figure 11. Control and indicator panel.



The graphs of cylinder pressure (bar) vs. crank angle (°) and cylinder pressure (bar) vs. cylinder volume (m<sup>3</sup>) are displayed on the chart panel at a data sampling rate of 0,1°.

## 8 MEASUREMENTS

### 8.1 CYLINDER PRESSURE MEASUREMENT

A piezoelectric pressure sensor mounted in the cylinder head and connected to a charge amplifier is used to measure the cylinder pressure. Cylinder pressure is measured using the trigger signal from encoder's zero pulse and at a sample rate (0,1°) provided by encoder output. Block diagram of cylinder pressure measurement is shown in Fig. 12.

### 8.2 AIR FLOW AND TEMPERATURE MEASUREMENTS

Air flow and inlet air temperature are measured with air mass flow meter (MAF). Its output signal is calibrated to 1,239-4,4578 V. for 8-480 kg/h. MAF's flow-output graph is shown in Fig. 13 and the fitted equation is given by equation 1.

$$Air\ Flow(kg / h) = -0,7165V^6 + 12,327V^5 - 82,178V^4 + 282,14V^3 - 508,88V^2 + 485,06V - 189,4$$

(1)

Figure 12. Block diagram of cylinder pressure.

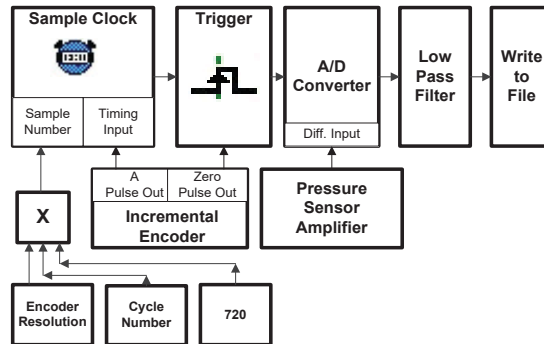
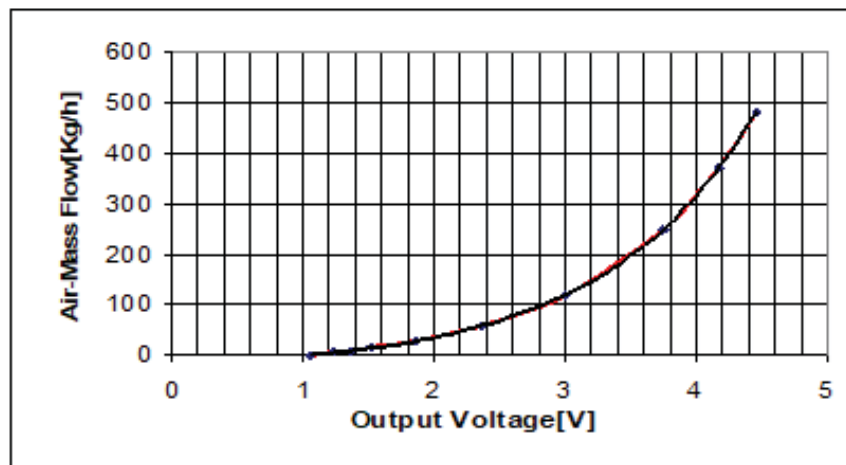


Figure 13. Graph of the MAF output measurement.



Since single cylinder diesel engine is used, some amount of suction air returns back to the surge tank again. Therefore, both suction and backward air flows are measured accurately to calculate the correct inflow to the cylinder. Suction signal frequency has to be the half of the engine speed frequency. Therefore, the MAF output is examined in frequency spectrum to realize filter for return signal. To measure inflow, low pass filter whose cut-off frequency is changed according to engine speed is added into the program. Cut-off frequency is adjusted between 8 and 25 Hz while engine speed frequency is between 16 and 50 Hz. A thermistor in the MAF is used with Wheatstone bridge to measure inlet air temperature. Frequency spectrum of MAF output is shown in

Fig. 13. The block diagram of air flow measurement is shown in Fig. 14.

Figure 14. Frequency spectrum of suction.

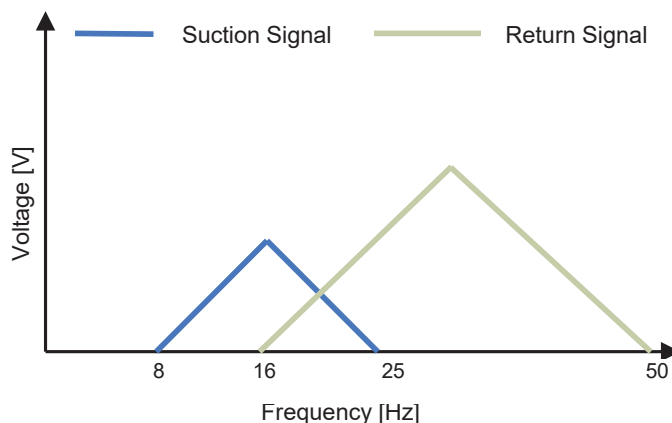
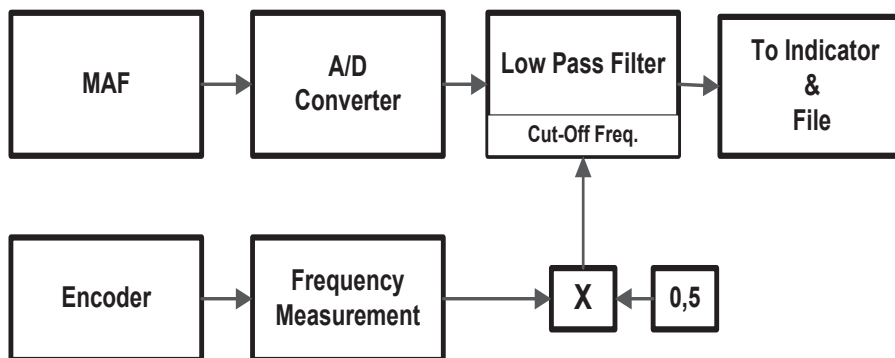


Figure 15. Block diagram of the air flow measurement and return flow signals.

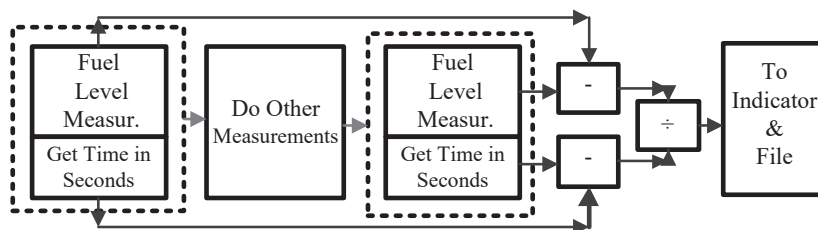


8.3 FUEL FLOW MEASUREMENT

To measure fuel flow, a level sensor is mounted in a cylindrical tank whose diameter is 5 cm and length is 75 cm. The level sensor is calibrated by measuring the mass of fuel and corresponding output voltage difference. The calibration values are shown in Table 5. The block diagram of fuel flow measurement is shown in Fig. 16.

Table 5 Calibration data of the level sensor

Δvoltage [v]	Δmass [g]	Sensitivity [v/g]	Mean Sensivity [v/g]
0,59	90,8	0,006479	0,00645
0,59	90,7	0,006504	
0,6	94,2	0,006369	

**Figure 16 Block diagram of the fuel flow measurement**

#### 8.4 TORQUE AND POWER MEASUREMENTS.

A loadcell is mounted to DC generator's frame to measure torque. Its technique is based on that armature current being consumed by load resistances is directly proportional to rotational force of field winding fixed generator body. Torque values are filtered by low pass filter whose cut-off frequency is 10 Hz to reduce noise due to engine vibration. Torque is calculated by multiplying the force on the loadcell and the arm length. Torque and power are calculated as follows:

$$\text{Torque(Nm)} = F_{\text{Loadcell}} \text{ (N)} \times \text{Arm Length(m)} \quad (2)$$

$$\text{Mechanical Power(kw)} = \frac{\text{Torque(Nm)} \times \text{Speed(rpm)}}{9550} \quad (3)$$

#### 8.5 ENGINE SPEED MEASUREMENT

Encoder's zero pulse is connected to counter/timer input of the data acquisition card to measure frequency. Zero pulse provides one pulse per revolution. The frequency value is multiplied by 60 to obtain engine speed as rpm. This final value is sent to the indicator chart and log file.

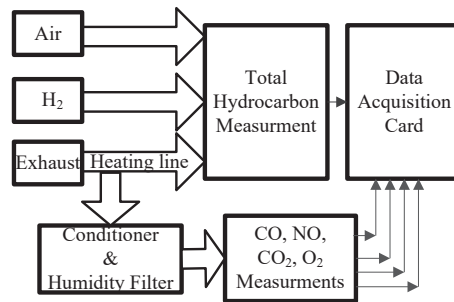
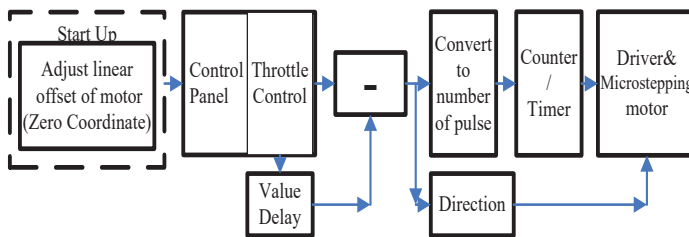
#### 8.6 EXHAUST EMISSION MEASUREMENT

Exhaust emissions are measured when engine conditions are adjusted by the graphical user interface. Emission values can be seen on the graphical user interface. The block diagram of emission measurement system is shown in Fig. 17.

### 9 CONTROLS

#### 9.1 THROTTLE CONTROL

Throttle is controlled by using micro stepping motor with linear actuator. The actuator is linked to the throttle pedal to move data acquisition card's counter/timer and digital output is connected to micro stepping motor driver to enable motion and its direction. The block diagram of the throttle control is shown in Fig. 18.

**Figure 17 Block diagram of the emission Measurement system.****Figure 18 Block diagram of throttle control system.**

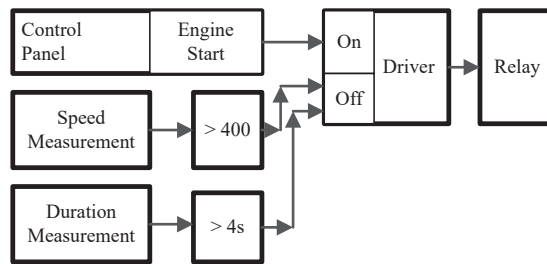
## 9.2 LOAD CONTROL

A resistance box is designed to load the engine. There are 16 resistances in the box and each of them has 1kw electrical power. All resistances are controlled as percent on the control panel. A 3 bit digital data is sent to decoder and the decoder activates required numbers of contactors' driver.

## 9.3 DIESEL ENGINE START/STOP CONTROL

A relay and its driver connected to data acquisition card are used to start the engine. Motor starter is energized by pressing the start button on the control panel, The starter motor is turned off automatically after 4 sec. to keep starter motor undamaged. A solenoid is connected to the engine's stop valve to stop the engine from the control room. When the solenoid is energized, it pulls the fuel valve and engine stops. The block diagram of Diesel engine start-stop control is shown in Fig. 19.

**Figure 19 Block diagram of the engine start control.**



## 10 RESULTS

The research facility is fully instrumented using a range of sensors and a computerized data processing and analysis system and it is capable of computing diesel engine performance characteristics. Results of measurements are obtained using the graphical user interface in the control room. With the help of user friendly properties of the graphical user interface, any further test procedures can be programmed. Sample measurement results are given in Table 6.

**Table 6 Sample measurements.**

Diesel Engine Measurements							
Speed	Torque	Power	Air Flow	Fuel Flow	Air/Fuel	Air Temp.	Load
1636 RPM	25,045 Nm	4,289 KW	39,143 Kg/h	1,675 Kg/h	23,36	25,9 °C	40%
Emission Measurements							
CO		NO <sub>x</sub>	CO <sub>2</sub>	O <sub>2</sub>	THC		
306,872 ppm		518,022 ppm	4,66%	14,35%	318,91 ppm		

Obtained data are in a good agreement with the engine manufacturer’s data. The maximum power of the diesel engine is 15 HP (11,19 kW) and as can be seen from Fig.20., the obtained maximum power from the diesel engine test rig at 2500 rpm under %60 load is 11,6 kW.

**Figure 20 Pressure (Bar) vs. CA(Deg) and Volume (m3) diagrams.**

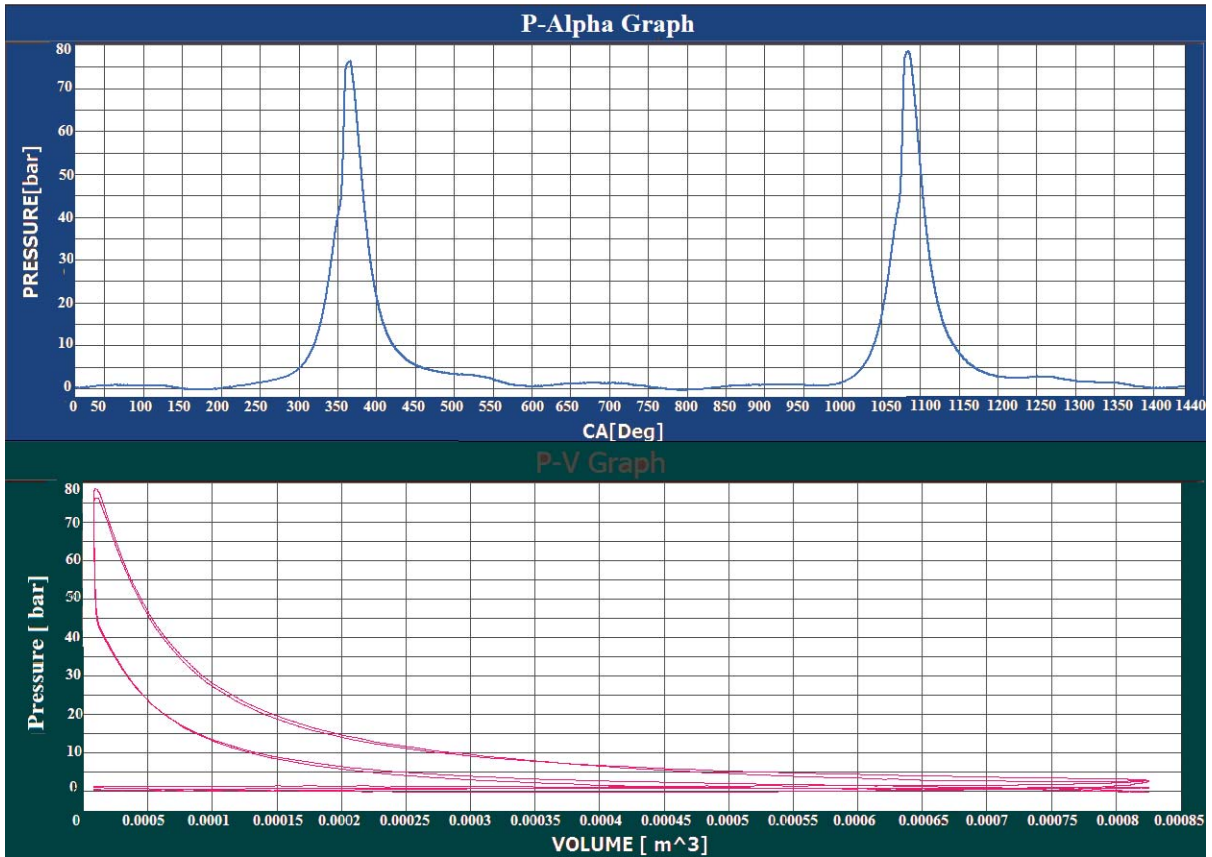


Figure 21 rpm versus power.

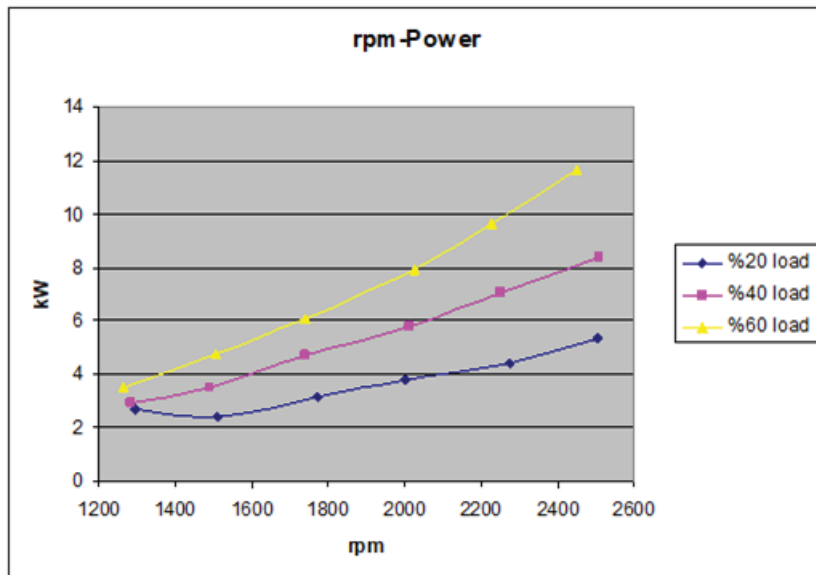


Figure 22 rpm versus NOx .

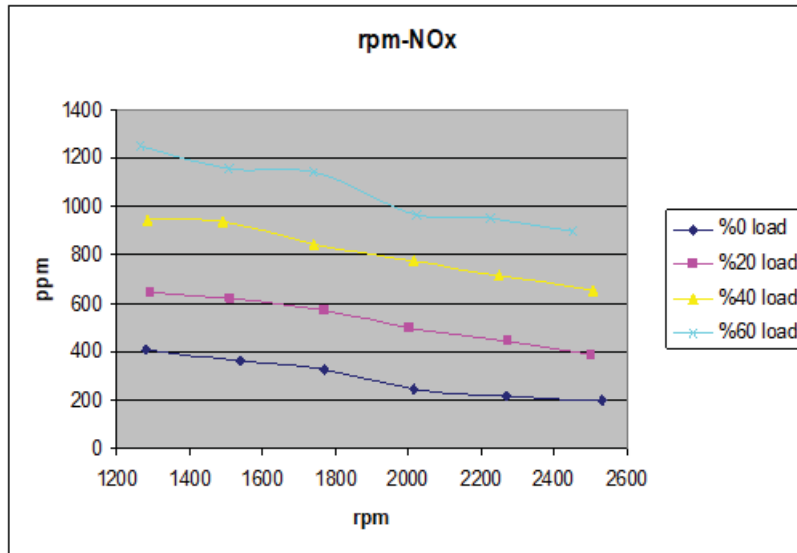


Figure 23 rpm versus CO2 .

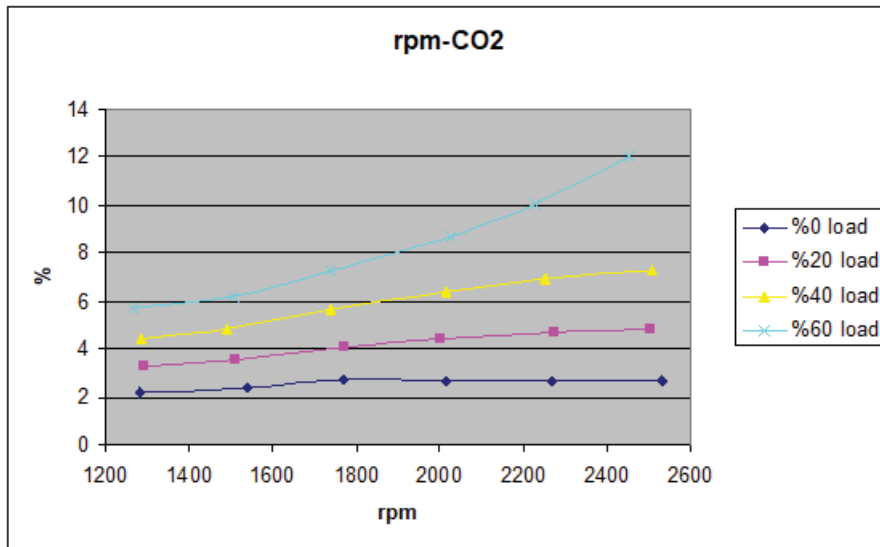
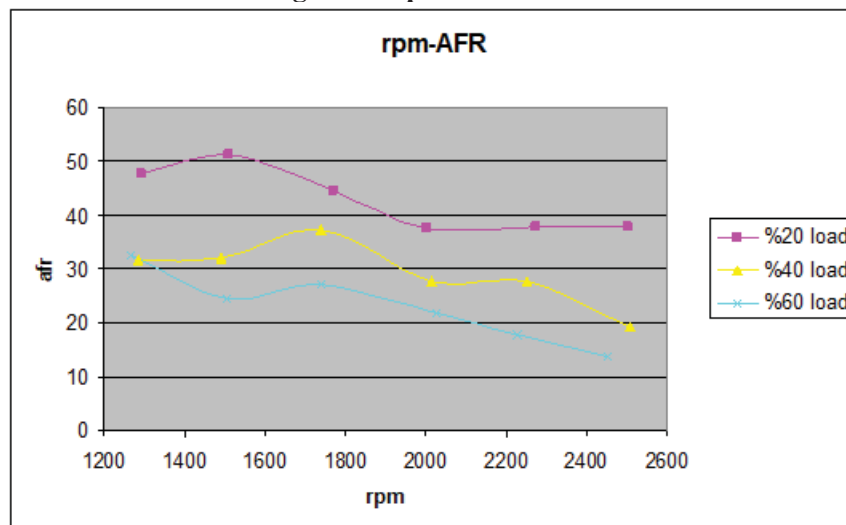


Figure 24 rpm versus AFR.



Also Figs. 22-23-24 show the variation of power with rpm and measured NO<sub>x</sub> and CO<sub>2</sub> exhaust emissions under variable engine speeds and loads. The effects of engine speed and load on air fuel ratio (AFR) can be seen from Fig.24.

In Section 6-10 above a computer controlled and fully instrumented ICE test facility which was designed and developed successfully at TUDEV/Piri Reis University was described. The engine laboratory is separated into two facilities, one holding the instrumented engine and the other computing and display units with a view to improve safety and to decrease exposure to noise. Analogue and digital control and measurement signals supplied by sensors and actuators in the engine room are conditioned and displayed on the graphical user interface using Labview® and logged by transferring signals from the engine room to the computerised engine control room. The facilities have proven to produce accurate and reliable experimental results at varying engine loads and speeds. The application of Labview and the engine software are novel features of the new engine rigs at TUDEV/Piri Reis. Therefore, noise of engine and the risk of injury have been decreased as well as convenient and safe laboratory environment has been provided. This physical model was matched with the mathematical model. Various design changes can be made to the rig and the mathematical model used then to project changes in engine behaviour. Alternatively, the mathematical model can be matched to any engine and then a series of change can be made using the model to predict changes in the engine performance and likely benefits. The actual engine tests can be found in Ziarati and Akdemir (2015) and similar results Ashok et al (2015). All test results were in line with Warsila's most recent gas engine results reported in 2018.

## 11 CONCLUSION

As can be seen the predicted theoretical values are in good agreement with the experimental results. The ability of the model to predict engine performance parameters of several engines of different type and sizes and considering the latest test on TUDEV Engine, to within the experimental error band (the instrumentation error range), for different test conditions must be considered very encouraging and a proof of the model. The air cycle used in the modelling of the engine is known as RZ Cycle which can represent any air standard cycle including diesel and gas or a combination. The Element Mixing Program can now be used reliably in establishing the effects of changes to running conditions or testing of changes to any given engine design parameters or to fuel injection equipment as well as to turbocharger configuration, and indeed to any other engine sub-system, without resorting to running the engine unnecessarily. This would reduce the cost of engine design and development to a minimum and allows changes to be introduced and their impact assessed while the engine itself is running without any changes made to it.

The model has used to study thermal efficiency; hybrid propulsion; alternative fuels, catalysts, exhaust recirculation systems; exhaust treatment; multi-Stage inter-cooling; variable geometry turbochargers, lighter materials; efficient bearings; water injection; novel injectors; high injection pressures, common rail systems. The next set of experiments is expected to study the application of quantum physics.

It is important note that the work in parallel and in addition to those reported above has been carried primarily to save fuel saving. Some of the methods used are listed below:

Slow steaming; Weather routing; Green energy – wind and sun (Flettner rotor & sun panels); Use of sea currents; e-navigation; Ballast water management; Hull and trim optimisation; Ship-port and port-ship system integration; Port-road-train-airport system integration; On-board ship management: such as AI and VR applications, Virtual arrival, advanced communications, JIT and predictive methods.

The results obtained to date can be considered very encouraging with substantial fuel savings and notable reductions in engine emissions.

The most important consideration is that diesel and gas combination is a feasible way forward for all diesel propulsion systems including ship engines which are invariably of diesel type. The reduction in emission of NO<sub>x</sub> and PMs were considerable and the results at high load conditions were better than with purely diesel fuel albeit it produced some adverse effect at low load conditions. The combination of gases with diesel as the ‘pre-igniter’ proved to enhance the brake thermal efficiency except that at mainly at part loads no improvements were observed. So, the results favours ship which often run at the design load and speed. Overall a mixture of gases as secondary fuel reduces the un-burnt hydrocarbon and produces less NO<sub>x</sub> and smoke at higher load conditions. The results cannot be published due to commercial restriction but good accounts of them are given in Ashok et al (2015).

#### References:

Ashok, B.; Ashok, D. S.; Kumar, C. R. LPG diesel dual fuel engine – a critical review. *Alexandria Engineering Journal*, Elsevier, 2015, **54**(2), 105-126. ISSN 1110-0168 . [Date of access: July 2020]. Available from: <<https://doi.org/10.1016/j.aej.2015.03.002>>.

Annand, W. J. D. Heat transfer in the cylinder of reciprocating internal combustion engines. *Proc. I. Mech. E.*, Sage Journals, 1963 **177**(1), 973-996. ISSN: 2058-1203. Available from: <[https://doi.org/10.1243/PIME\\_PROC\\_1963\\_177\\_069\\_02](https://doi.org/10.1243/PIME_PROC_1963_177_069_02)>.

Campbell, T.; Galbraith, J. Development of a low cost microcomputer system for data acquisition and control of a diesel engine test bed facility. *Int. J. of Vehicle Design*. Genève: Inderscience Pub., 1985, **6**(4-5). ISSN 1741-5314 . Available from: <<https://doi.org/10.1504/IJVD.1985.061411>>.

Celik, M.; Bahattin, Bayır, R.; Özdalyan, B. Bilgisayar Destekli Motor Test Standının Tasarımı ve İmalatı. *Teknoloji*. 2007, **10**(2), 131-141.

Ferguson C. R. *Internal combustion engines: applied thermosciences*. New York: John Wiley & Sons Inc., 1986.

Gilchrist, J. M. Chart for the investigation of thermodynamic cycles in internal combustion engines and turbines. In: *Proc. I. Mech. E.* Thousand Oaks: Sage Journals, 1947, **159**(1), 335-349. ISSN 2058-1203. Available from: <[https://doi.org/10.1243/PIME\\_PROC\\_1948\\_159\\_027\\_02](https://doi.org/10.1243/PIME_PROC_1948_159_027_02)>.

Glauert, M. B. The Wall Jet. *J. Fluid Mech.* Cambridge University Press, 1956, 1, 625-643. Available from: <<http://dx.doi.org/10.1017/S002211205600041X>>.

Heywood, J. B. *Internal Combustion Engine Fundamentals*. Singapore: McGraw-Hill Education, 1988. McGraw Hill Series in Mechanical Engineering. ISBN 978-0070286375.

Kawarabayash, S.; Fujii, T. Design of optimal servo system for engine test bed by ILQ method. In: *Proceedings of the 29th. IEEE Conference on Decision and Control*. Honolulu: IEEE, 1990, 3, 1579-1583. Available from: <DOI:10.1109/CDC.1990.203879>.

Mert, A.; Ozkaynak, S.; Ziarati, R. et al. *Design and development of a computer controlled marine diesel engine facility for maritime engineering research and training*. Warwickshire: International Maritime Lecturers Association, 2009. [Date of access: July 2020]. Available from: <[http://www.marifuture.org/Publications/Papers/IMLA\\_09\\_Engine\\_Paper.pdf](http://www.marifuture.org/Publications/Papers/IMLA_09_Engine_Paper.pdf)>.

Brunt, M. and Platts, K. Calculation of heat release in direct injection diesel engines. *SAE Technical Paper 1999-01-0187*. 1999. ISSN:0148-7191. Available from: <<https://doi.org/10.4271/1999-01-0187>>.

Ozkaynak, S. *MPhil/PhD Transfer Report*. TUDEV, 2009.

Ozkaynak, S.; Ziarati, R.; Bilgili, E. Design and development of a diesel engine computer simulation program. In: *13<sup>th</sup> Congress of Intl. Maritime Assoc. of Mediterranean: IMAM 2009: İstanbul, Turkey, 12-15 October*. Istanbul: IMAM, 2009.

Plint, M.; Martyr, A. *Engine testing, theory and practice*. Oxford: Butterworth, 1999.

Rillings, James H.; Creps, Wendell D.; Vora, Lakshmi S. A Computer-controlled engine test cell for engineering experiment. In: *Proceedings of the IEEE*. IEEE, 1973, 61(11), 1622-1626. ISSN:1558-2256. Available from: <DOI:10.1109/PROC.1973.9335>.

Schmidt, M. Extended vehicle model for dynamical engine test stands. In: *Proceedings of the 1998 American Control Conference*. IEEE, 1998, 4, 2268-2271. ISSN 0743-1619. Available from: <DOI:10.1109/ACC.1998.703031>.

Travis, J.; Kring J. *Labview for everyone: graphical programming made easy and fun*. 3rd Edition. Pearson Education Inc., 2007.

Turley, P.; Wright, M. Developing engine test software in LabVIEW®. In: *1997 IEEE Autotestcon Proceedings AUTOTESTCON '97. IEEE Systems Readiness Technology Conference. Systems Readiness Supporting Global Needs and Awareness in the 21st Century*. IEEE, 1997. 575-579. ISBN 0-7803-4162-7. Available from: <DOI:10.1109/AUTEST.1997.633678>.

UdayaKumar R.; Anand M.S. Multizone combustion model for a four stroke direct injection diesel engine. *SAE Technical Paper 2004-01-0921*, 2004. ISSN 2688-3627. Available from: <<https://doi.org/10.4271/2004-01-0921>>.

Void, K.U. A control scheme for a dynamic combustion engine test stand. In: *International Conference on Control 1991. Control '91*. IEEE, 1991. 2, 938-943. ISBN 0-85296-509-5.

Williamson, A.C.; Al-Khalidi, K.M.S. An improved engine-testing dynamometer. In: *1989 Fourth International Conference on Electrical Machines and Drives*. IET, 1989. 374-378. ISBN 0537-9989.

Ziarati, R. Engine performance analysis using mathematical modelling. *Bryce International, Report No: 81-TN-55*. 1991

Ziarati, R.; Akdmir, B. LeanShip - design and development of a high fidelity integrated ship management system for matching engine operations to sea and air conditions. In: *Conference: AVTECH '15 - Automotive and Vehicle Technologies Conference*. Istanbul, 2015.

Ziarati, R., *Design and use of hybrid vehicles*. Natinion Lecture and Paper. IRTE, 1995. [Awarded the Mackenzie Junner Award 1995 for best National Lecture and the National Diploma for Best Paper 1996].

Ziarati, R.; Veshagh, A. Mathematical modelling and computer simulation of medium size diesel engine running of varying quality fuels. In: *International Symposium COMODIA 90*. Kyoto, 1990. 587-594. [Date of access: July 2020]. Available from: <[https://www.jsme.or.jp/esd/COMODIA-Pros/Data/002/C90\\_P587.pdf](https://www.jsme.or.jp/esd/COMODIA-Pros/Data/002/C90_P587.pdf)>.

Ziarati, R.; Veshagh, A.; Hawksley, G. *Fuel sprays interaction and combustion modelling*. EC Non-Nuclear Research Programme (and Lloyds Register) Report. 1988